

Decision-Oriented Intervention Cost Prediction for Multi-robot Persistent Monitoring

Guangyao Shi, Chak Lam Shek, Nare Karapetyan, Pratap Tokekar

Abstract—In this paper, we present a differentiable, decision-oriented learning technique for a class of vehicle routing problems. Specifically, we consider a scenario where a team of Unmanned Aerial Vehicles (UAVs) and Unmanned Ground Vehicles (UGVs) are persistently monitoring an environment. The UGVs are occasionally taken over by the humans to take detours to recharge the depleted UAVs. The goal is to select routes for the UGVs so that they can efficiently monitor the environment while reducing the cost of interventions. The former is modeled as a monotone, submodular function whereas the latter is a linear function of the routes of the UGVs. We consider a scenario where the former is known but the latter depends on the context (e.g., wind and terrain conditions) that must be learned. Typically, we first learn to predict the cost function and then solve the optimization problem. However, the loss function used in prediction may be misaligned with our final goal of finding good routes. We propose a *decision-oriented learning* framework that incorporates task optimization as a differentiable layer in the prediction phase. To make the task optimization (which is a non-monotone submodular function) differentiable, we propose the Differentiable Cost Scaled Greedy algorithm. We demonstrate the efficacy of the proposed framework through numerical simulations. The results show that the proposed framework can result in better performance than the traditional approach.

I. INTRODUCTION

Vehicle Routing Problems (VRP) have been commonly studied over the years [1], especially in the context of using Unmanned Aerial Vehicles (UAVs) for persistent monitoring of an environment [2]. Typically, the route planning is solved as a combinatorial optimization problem. The objective typically involves several parameters (e.g., cost of executing a route), which are assumed to be known. In practice, actual parameters may be unknown and may depend on the context (e.g., environmental factors). Traditionally, we solve this in two phases: first, we learn the parameters using historical data and then plug the learned parameters into the route optimization algorithm.

Recent work has shown that this two-phase approach may be unnecessary and, in some cases, sub-optimal [3]–[6]. Particularly, a good prediction of the parameters may be sufficient but unnecessary in making good route decisions. Further, the *loss* function used in learning to predict the parameters may be misaligned with the downstream task (i.e., finding good routes). An alternative is to solve this problem end-to-end, where we directly map the context input to the routes using, for example, deep neural networks. The

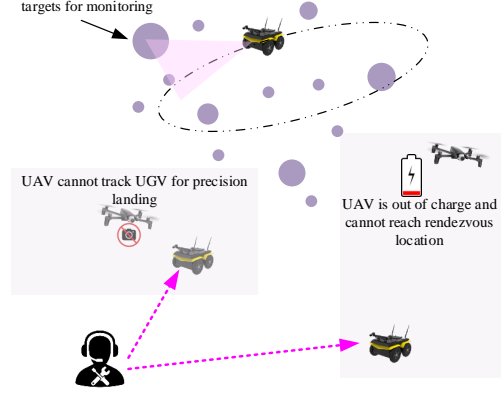


Fig. 1. The motivating case study of Intervention-aware UGVs routing.

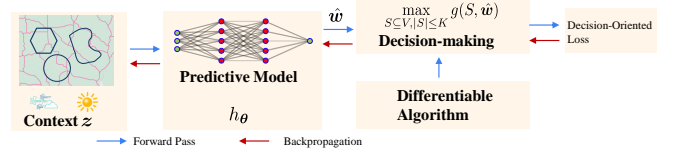


Fig. 2. The proposed framework that incorporates the non-monotone submodular maximization into the learning process.

objective in such an approach is not misaligned since the loss function for training the network will depend directly on the routes selected. However, such an approach faces two limitations. Training end-to-end a combinatorial optimization problem may require a lot of data [7]. Further, the black-box nature of neural networks will make the route selection hard to explain or interpret. Instead, we focus on a *Decision-Oriented Learning* (DOL) framework, as shown in Fig. 2, that achieves the best of both worlds. We treat the combinatorial optimization problem as a layer in the learning pipeline. By making the optimization differentiable, we can train the prediction network using the downstream route loss rather than prediction loss. Our results demonstrate that this approach leads to better route selection than the two-phase traditional approach.

In this paper, we consider a specific VRP scenario where a team of UAVs along with a team of Unmanned Ground Vehicles (UGVs) are persistently monitoring an environment (Fig. 1). The UAVs occasionally land on the UGVs for recharging.

However, due to the uncertainty inherent in the environment, failures and malfunctions are inevitable. For example, as shown in Fig. 1, the tracking camera of a UAV may

This work is supported in part by National Science Foundation Grant No. 1943368 and Army Grant No. W911NF2120076.

Authors are with the University of Maryland, College Park, MD 20742 USA [gyshi, cshek1, knare, tokekar]@umd.edu

stop working, and it may not reliably land on the UGV for recharging. Likewise, the UAV may end up out of charge before reaching the UGV due to the stochastic wind field. In such cases, the human operator may have to intervene to recover the UAV (either by directly going to the UAVs location or by teleoperating the UGV to get to the UAV). Each intervention is costly as it requires the human operator's attention and causes an interruption to the monitoring task. We need to account for the cost of intervention in the route selection.

The intervention cost depends on the UAV and UGV routes as well as the environmental factors (e.g., wind conditions). We call all these factors together as *context*. We are interested in finding such a mapping from context observation to the intervention cost.

We consider the optimization objective to be a combination of the monitoring performance and the intervention cost. The monitoring performance is a monotone, submodular function for which a greedy algorithm yields a constant-factor approximation [8]. In our recent work, we presented a DOL framework for differentiable submodular maximization of monotone functions. However, by including the intervention cost in the objective, we cannot guarantee that the objective is monotone or even non-negative anymore. To accommodate such non-monotone optimization, we present a Differentiable Cost-Scaled Greedy (D-CSG) algorithm. The differentiability of the non-monotone submodular maximization is achieved by using the multi-linear extension of the set function along with a novel differentiable algorithm, which expands and approximates the existing non-differentiable algorithm [9] as a differentiable computational graph.

In sum, our contributions include:

- Propose a novel differentiable algorithm (D-CSG) based on the Cost-Scaled Greedy (CSG) algorithm.
- We propose a decision-oriented learning framework for predicting intervention costs.
- We demonstrate the effectiveness of our framework in several examples through simulation.

II. RELATED WORK

Many existing works are considering the routing problem of the UGVs as mobile recharging stations [10], [11]. The routing problem involves actively planning routes to assist UAVs in recharging tasks. By contrast, in our motivating case study, the recharging process happens passively (UAVs will autonomously reach the UGV when they need to), and the UGVs focus on their own coverage tasks but may be interrupted. Besides, different from the existing work that assumes a known objective, our work admits the fact that the parameters in the objective function (intervention costs) may vary from context to context, for example, in different weather conditions, and aims at learning a context-aware objective.

Another line of research related to this work is decision-oriented learning. The central concept involves the incorporation of decision-making challenges as differentiable layers within the learning pipelines. This approach presents

a notable advantage in enabling end-to-end training while mitigating the need for extensive engineering efforts in formulating intermediate learning objectives. Its inception traces back to its initial exploration within the context of continuous optimization problems, as evidenced by previous works such as [12] and [13]. Subsequently, this concept has garnered significant traction within the fields of control and robotics [14]–[17]. Furthermore, the concept has been extended to encompass combinatorial problems like [3]–[5], [18]. Our present research draws inspiration from the approaches outlined in [3] and [4]. Our proposed framework seamlessly integrates the decision-making process for Intervention-aware UGV routing, formulated as a non-monotone submodular maximization problem, into the learning process.

This work is also closely related to differentiable submodular maximization. Submodular maximization and its various adaptations have found widespread application in multi-robot decision-making scenarios encompassing tasks such as coverage, target tracking, exploration, and information gathering. These studies all benefit from the greedy algorithm and its variants that can solve submodular maximization problems efficiently with a provable performance guarantee. Since the submodular objective and greedy algorithm are tightly coupled, it is better to consider the influence of the greedy algorithm when we consider learning submodular functions [19]. For the non-monotone submodular objective considered in this paper, the simple greedy algorithm [8] does not have a performance guarantee, and we need to use a variant called the CSG algorithm to maximize the objective. As a result, the differentiable versions of the simple greedy algorithm [19], [20] cannot be directly used in our learning framework, and we need to develop our differentiable version of the CSG algorithm. Besides, our D-CSG algorithm is technically different from the existing differentiable greedy algorithm. The approach in [19], [20] is based on adding stochastic disturbances to the algorithm and using a gradient estimator. Our algorithm is based on the relaxation of the non-differentiable operation to a differentiable operation and the relaxation of the set function to a continuous counterpart.

III. PRELIMINARIES

A. Submodular Set Functions

The formal definition of a submodular function is given below.

Definition 1 (Submodularity). For a set \mathcal{V} , a function $f : \{0, 1\}^{\mathcal{V}} \mapsto \mathbb{R}$ is submodular if and only if for any sets $\mathcal{A} \subseteq \mathcal{V}$ and $\mathcal{A}' \subseteq \mathcal{V}$, we have $f(\mathcal{A}) + f(\mathcal{A}') \geq f(\mathcal{A} \cup \mathcal{A}') + f(\mathcal{A} \cap \mathcal{A}')$.

Let $f : \{0, 1\}^{\mathcal{V}} \rightarrow \mathbb{R}_{\geq 0}$ and $c : \{0, 1\}^{\mathcal{V}} \rightarrow \mathbb{R}_{\geq 0}$ be a normalized monotone submodular function and a non-negative linear function, respectively. We are interested in a special type of submodular function $g : \{0, 1\}^{\mathcal{V}} \rightarrow \mathbb{R}$, which is defined as

$$g(\mathbf{x}, \mathbf{w}) = f(\mathbf{x}) - \lambda c(\mathbf{x}, \mathbf{w}), \quad (1)$$

where \mathbf{w} is cost vector for the set \mathcal{V} ; $\mathbf{x} \in \{0, 1\}^{\mathcal{V}}$; λ is a user-specified parameter for their cost tolerance level; and

$$c(\mathbf{x}, \mathbf{w}) = \mathbf{w}^T \mathbf{x}.$$

It should be noted that g is still a submodular function, but it can take both positive and negative values and may not be monotone [9], [21]. Such a function is suitable to model the scenario where we need to balance the task performance ($f(\mathbf{x})$) with the cost needed to achieve the performance ($c(\mathbf{x}, \mathbf{w})$).

The decision-making is to solve the following problem:

$$\begin{aligned} \max_{\mathbf{x} \in \{0,1\}^V} g(\mathbf{x}, \mathbf{w}) \\ \text{s.t. } \mathbf{1}^T \mathbf{x} \leq K, \end{aligned} \quad (2)$$

where K is the number of elements that can be selected.

B. Case Study: Intervention-Aware UGV Routing

As described earlier, we consider the case of UAVs and UGVs persistently monitoring the environment with occasional interventions to recover the nonoperational UAVs. We focus on selecting the routes for $n_g = K$ UGVs and assume that the UAV routes are fixed. Specifically, we consider that we are given a set of candidate routes, \mathcal{T} , and we need to select a subset from \mathcal{T} for the UGVs. Here, \mathcal{T} corresponds to the ground set \mathcal{V} . For any subset $S \in \mathcal{T}$, $f(S)$ gives the weighted coverage achieved by the UGVs executing the routes in S . Similarly, $c(S, \mathbf{w})$ gives the expected cost of intervention for the selected routes S where \mathbf{w} are the unknown cost vectors. The objective then is:

$$\max_{S \in \mathcal{T}} g(S, \mathbf{w}) \quad (4)$$

$$\text{s.t. } |S| \leq K. \quad (5)$$

We observe that this is the same problem as described earlier in Eq. 2.

The cost $c(S, \mathbf{w})$, i.e., how often and how much time we expect the human operators to be involved are closely related to how fast the UAVs consume energy and how close the UAVs and UGVs will be to each other when a recharging rendezvous is needed. From the UGVs' remote supervisor's perspective, some routes can cover many import task locations, but the UGV may be interrupted frequently to assist the UAVs. Since we plan the routes before knowing if/when/where the interventions will need to occur, our combined objective $g(S)$ aims to achieve a balanced performance between task coverage by the UGVs and expected human intervention costs.

We can compute the intervention cost if we know the value of cost vector \mathbf{w} . If \mathbf{w} is known, we can solve problem (2) using the existing algorithm [9]. However, in practice, we do not know the intervention cost in advance when we make decisions. Instead, we have some indirect information. We call the latter as *context* \mathbf{z} , which can include the geometric information of the routes of the UAVs and UGVs, the environmental conditions (e.g., wind conditions), etc. Hence, we solve two problems (simultaneously): predicting \mathbf{w} from \mathbf{z} and using the predicted \mathbf{w} to find routes S by solving Eq. 2.

IV. PROBLEM FORMULATION

Our goal is to learn a function $h_\theta : \mathcal{Z} \rightarrow \mathbb{R}_+^N$ that maps the context observation $\mathbf{z} \in \mathcal{Z}$ to the objective parameters $\mathbf{w} \in \mathbb{R}_+^N$. Traditionally, finding the mapping h_θ and optimizing the downstream objective $g(S, \mathbf{w})$ are considered separately: given the training data $\mathcal{D} = \{(\mathbf{z}_1, \mathbf{w}_1), (\mathbf{z}_2, \mathbf{w}_2), \dots, (\mathbf{z}_{|\mathcal{D}|}, \mathbf{w}_{|\mathcal{D}|})\}$, find the mapping h_θ by optimizing over θ in a supervised fashion. After optimization, use the parameter $\mathbf{w} = h_\theta(\mathbf{z})$ for decision-making (solve Eq. (2)) when we get an observation \mathbf{z} .

However, in robotic applications, the available training data is usually limited. Such a pipeline may result in a h_θ that either overfits the data or cannot generalize well when deployed, i.e., leads to low-quality decisions in the downstream task. At a high level, the question that we will explore in this paper is:

Can we improve the decision quality in the downstream tasks if we explicitly incorporate the downstream optimization into the process of learning h_θ ?

Our answer is that optimizing the following decision-oriented loss can improve the decision quality compared to the baseline approach.

Decision-Oriented Loss: for a given training data $(\mathbf{z}_i, \mathbf{w}_i)$, the decision-oriented loss $\ell_{DOL}(\mathbf{w}_i, \hat{\mathbf{w}}_i)$ is defined through Eq. (6) to Eq. (8):

$$\hat{\mathbf{w}}_i := h_\theta(\mathbf{z}_i) \quad (6)$$

$$\hat{\mathbf{x}} := \mathbf{x}^*(\hat{\mathbf{w}}_i) \text{ solving (2) with } \mathbf{w} = \hat{\mathbf{w}}_i \quad (7)$$

$$\ell_{DOL}(\hat{\mathbf{w}}_i, \mathbf{w}_i) := g(\mathbf{x}^*(\mathbf{w}_i), \mathbf{w}_i) - g(\hat{\mathbf{x}}, \mathbf{w}_i), \quad (8)$$

where $\mathbf{x}^*(\mathbf{w}_i)$ denotes the solution of (2) returned by some approximation algorithms with $\mathbf{w} = \mathbf{w}_i$; $g(\mathbf{x}^*(\mathbf{w}_i), \mathbf{w}_i)$ denotes the decision quality when we use the ground truth parameter \mathbf{w}_i for decisions; $g(\hat{\mathbf{x}}, \mathbf{w}_i)$ denotes the decision quality when we use the predicted parameter $\hat{\mathbf{w}}_i$ for decisions, i.e., use $\hat{\mathbf{w}}_i$ to obtain the decision $\hat{\mathbf{x}}$, but the decision is evaluated w.r.t. the true parameter \mathbf{w}_i .

The intuition for Eq. (8) is that we want to minimize the gap between the decision quality of the true parameters and that of the predicted parameters. One challenge is when we use the chain rule to compute the gradient of the loss function we need to differentiate through the optimization problem (the first term on the r.h.s. of Eq. (9)) as shown in the illustrative computational graph in Fig. 2.

$$\frac{\partial \ell_{DOL}}{\partial \theta} = \frac{\partial \ell_{DOL}}{\partial \hat{\mathbf{w}}_i} \cdot \frac{\partial \hat{\mathbf{w}}_i}{\partial \theta} \quad (9)$$

In the following sections, we will show how to approximately compute the first term on the r.h.s. of Eq. (9).

V. LEARNING ALGORITHM

This section will explain the differentiable algorithm used in our decision-oriented learning framework.

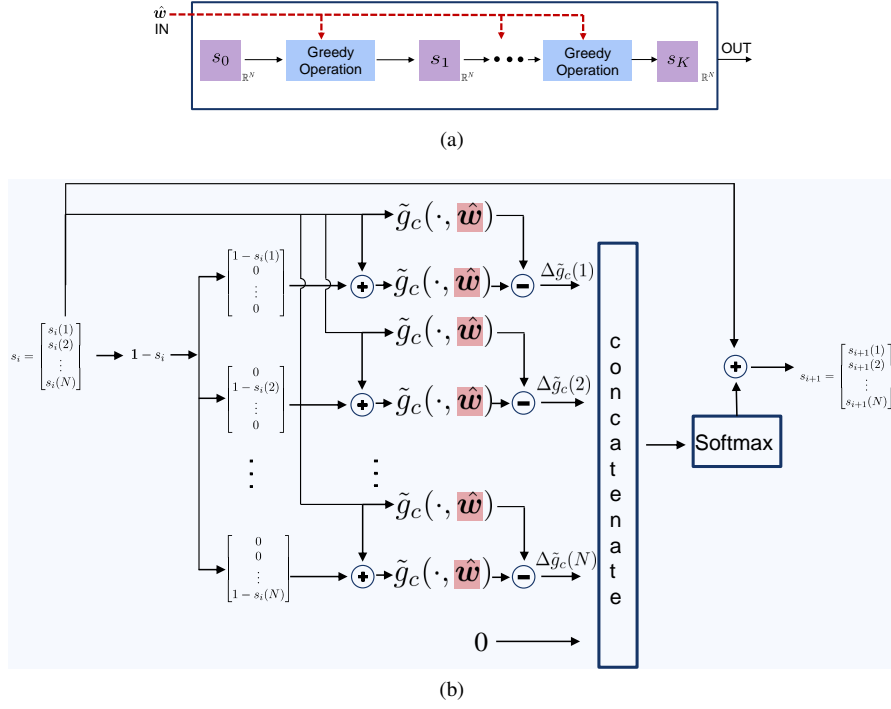


Fig. 3. Computational graph of the proposed differentiable algorithm. (a) The structure of the algorithm. (b) The internal structure of the differentiable cost-scaled greedy operation.

Algorithm 1: Cost-Scaled Greedy (CSG) Algorithm

Input : Ground set V , scaled objective

$\tilde{g}(S, \mathbf{w}) = f(S) - 2c(S, \mathbf{w})$, cardinality K

Output: A set $S \subseteq V$

```

1  $S \leftarrow \emptyset$ 
2 for  $i=1$  to  $K$  do
3    $e_i \leftarrow \operatorname{argmax}_{e \in V} \tilde{g}(e \mid S)$ 
4   if  $\tilde{g}(e_i \mid S) \leq 0$  then
5     break
6   end
7    $S \leftarrow S \cup \{e_i\}$ 
8 end
9 return  $S$ 

```

A. Cost-Scaled Greedy (CSG) Algorithm

The classic greedy algorithm cannot provide a performance guarantee for the objective in Eq. (1). Instead, a modified version of the greedy algorithm, CSG, was proposed in [9] and was shown to achieve an approximation satisfying that $f(Q) - c(Q, \mathbf{w}) \geq \frac{1}{2}f(OPT) - c(OPT, \mathbf{w})$, where Q is the solution returned by Algorithm 1 and OPT refers to the optimal solution. It should be noted that the output of such an algorithm is not differentiable w.r.t. the parameter \mathbf{w} .

B. Multilinear Extension of Submodular Function

A prerequisite for D-CSG to work is that we need to have a continuous and differentiable relaxation of the objective in Eq. (2). The linear part, $c(\mathbf{x}, \mathbf{w})$, can be directly relaxed to a continuous version. As for the submodular part, $f(\mathbf{x})$, We

use the multilinear extension to relax the submodular part.

For a submodular function $f : \{0, 1\}^N \rightarrow \mathbb{R}_{\geq 0}$, its multilinear extension $F : [0, 1]^N \rightarrow \mathbb{R}_{\geq 0}$ is defined as

$$F(\mathbf{x}) = \sum_{S \subseteq \mathcal{T}} f(S) \prod_{i \in S} x_i \prod_{i \notin S} (1 - x_i), \quad (10)$$

which is a unique multilinear function agreeing with f in the vertices of the hypercube $[0, 1]^N$.

Let \mathbf{q} denote a random vector in $\{0, 1\}^N$, where each coordinate is independently rounded to 1 with probability x_i or 0 otherwise. It can be shown that the derivative $\frac{\partial F}{\partial x_i}$ is

$$\frac{\partial F}{\partial x_i} = \mathbb{E}_{\mathbf{q} \sim \mathbf{x}} [f([\mathbf{q}]_{i=1})] - \mathbb{E}_{\mathbf{q} \sim \mathbf{x}} [f([\mathbf{q}]_{i=0})], \quad (11)$$

where $[\mathbf{q}]_{i=1}$ and $[\mathbf{q}]_{i=0}$ are equal to the vector \mathbf{q} with the i -th coordinate set to be 1 and 0, respectively.

C. Differentiable-Cost-Scaled Greedy (D-CSG) Algorithm

Based on the CSG algorithm, we developed one differentiable version of CSG. The key idea is to expand the computation steps as one computational graph, as shown in Fig. 3a. Suppose we must select up to K elements from a ground set whose size is N . We abstract the CSG algorithm as a K step computational graph as shown in Fig. 3a. The selection vector is initially an all-zero vector, i.e., $s_0 = \mathbf{0}, s_0 \in \mathbb{R}^N$. In each step, the greedy operation will try to set one element in the selection vector from 0 to 1 approximately. The details of the greedy operation are given in Fig. 3b. For an input vector s_i , we must first identify the elements that are not selected yet by doing $1 - s_i$. Then, we separate $1 - s_i$ into N vectors, each of

which has one element from $1 - s_i$ and the rest is zero. Each vector represents selecting an element from what is left in the ground set. If an element $s_i(j) \approx 1$ (j is already selected), $1 - s_i(j)$ is approximately zero, and the sum of this vector with s_i implies adding no new element to s_i . By contrast, if an element $s_i(j) \approx 0$ (j is not selected yet), $1 - s_i(j)$ is approximately one, and the sum of this vector with s_i implies adding one new element to s_i . Then, we feed the selection result to the continuous relaxation of the cost-scaled objective function, \tilde{g}_c , to compute the marginal gain. To account for the branch control in Algorithm 1 (line 4-6), we add one dummy element with zero marginal gain when we concatenate all the marginal values. Then, this concatenated vector will be fed into one argmax operator to select the one with the largest marginal gain (similar to line 3 in Algorithm 1). If all the marginal gains are less than zero, then the output of the argmax will choose the dummy element. As a result, the first N elements of the output of the argmax will all approximately be zero, and the last element corresponding to the dummy selection will be one. Therefore, if we add the result of the first N elements to s_i to get a new N -dimensional vector, s_{i+1} , the s_{i+1} will be the same as s_i , which is in effect equivalent to skipping selection in this step. Such skipping step will also happen in the following steps since all marginal gains will be less than zero. It is equivalent to the branch control statement in Algorithm 1 (lines 4-6). It should be noted that the argmax operator itself is not differentiable and cannot be used during training. Instead, we use Gumbel-softmax [22], which uses a temperature parameter τ to scale how it is close to the argmax operator. A larger τ will make the approximate smoother, but the approximation error will also be larger. In experiments, this parameter is set empirically.

Remark 1. The greedy operation has two non-matrix operations: evaluation of \tilde{g}_c ($2N$ times) and softmax. The latter is much faster than the former. As a result, the time for evaluation of \tilde{g}_c will dominate the forward pass the greedy operation.

VI. EXPERIMENTS

In this section, we will evaluate the performance of the proposed framework for intervention cost prediction using synthetic data. We will first compare the performances of different algorithms to solve the randomly generated instances of Problem (2) to show the necessity and correctness of the D-CSG algorithm. Then, we will present one qualitative example of why the proposed framework is better than the classic one based on MSE loss. Next, we will present some quantitative results to show that the proposed framework leads to better decisions.

A. Simulation Setup

There are n_a UAVs and n_g UGVs. The global wind ω is represented as $[a, b, \omega_o]$, where a and b are the shape and scale parameters of Weibull distribution [23], respectively, and ω_o is the wind direction.

UAV and UGV Behavior: We consider the case that each task route of UAVs and UGVs is a circle, whose center is $[C_x, C_y]$ and radius is r . This geometric information can represent each route as a vector $[C_x, C_y, r]$. Our framework is also applied to more general types of task routes as long as we have a compact representation. We use circular routes for simplicity. Both vehicles need to monitor their assigned task routes persistently. Our main focus is on the UGV's side. As shown in Fig. 1, several targets of different values are scattered in the environment. The team of UGVs needs to cover some of them persistently. The team can get that value of the target if a target is covered by one UGV when the UGV traverses along the task route (when two or more UGVs cover a target, we can only get the value once). The team of UGVs will try to get a higher value in sum. At a high level, the team is trying to maximize a generalized coverage function [24], which is submodular. As for the UAVs, when the UAV is about to be out of charge, i.e., the state of charge drops below 30%, it will fly toward the closest UGV. We use the same energy model as that in [25] with a stochastic wind model. If it can successfully rendezvous with the UGV, it will be recharged. If it has to land before it can rendezvous with the UGV. In such a case, a human operator must take over until all vehicles return to their tasks.

Raw Data: Based on the UAV UGV behavior models, we build a simulator for the routing problems as in our previous work [6], [26], [27]. Given simulation parameters (e.g., UAV and UGV routes and wind conditions, λ), it will simulate vehicles' execution of persistent tasks. Based on this simulator, we randomly generate a set of context observations, and for each context z_i , there are a set of candidate task routes, \mathcal{T}_i , for UGVs. The size of \mathcal{T}_i is fixed to be N . Then, we will get the data by making a team of n_g UGVs execute different combinations of routes: collect simulation data and compute a corresponding w_i (average intervention time in minutes per hour) for z for all routes in \mathcal{T}_i . Such a process is repeated many times to generate the training data. In the test phase, we generate a set of context observations and test the performance of the algorithm by directly running the simulator.

B. Results for D-CSG Algorithm

We test the performance of the proposed differentiable algorithm in synthetic instances of the problem in (2). We compare with two baselines: one is the Naive Greedy [8] and CSG.

Objective Value For each instance, we set the objective value returned by CSG as the denominator and scale the outputs of D-CSG and NG. As shown in Fig. 5, our D-CSG achieves comparable performance compared to CSG, which suggests that the differentiability does not sacrifice much optimization performance. By contrast, the performance of the NG is, on average, worse than that of D-CSG, which justifies our motivation to develop a novel differentiable algorithm rather than using the differentiable version of NG.

Running Time The price of differentiability is mainly reflected in the running time. In experiments, we observe that

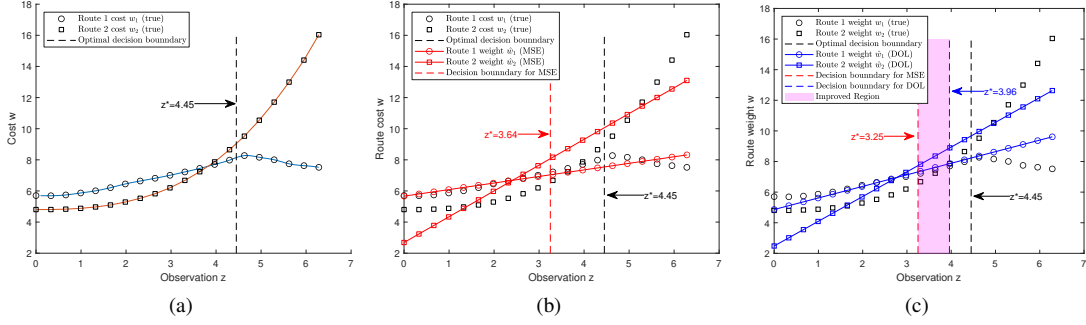


Fig. 4. A case study with three candidate routes and two UGVs. (a) Application scenario. (b) Ground truth data and the optimal decision boundary. (c) Learned linear models using MSE loss. (d) Learned linear models using the DOL framework.

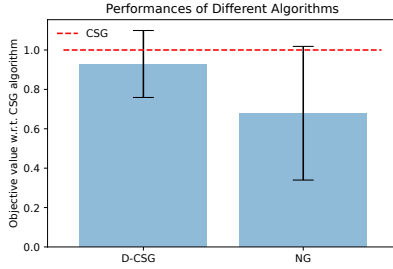


Fig. 5. Simulation results for the network (D-CSG).

the D-CSG is usually 20-30 times slower than CSG. This is mainly because the evaluation of the continuous relaxation of the submodular objective is time-consuming, which can be viewed as a polynomial with exponentially many terms w.r.t. the size of the route set. The running time can be improved by using an estimator for function evaluation and gradient computation [28]. We leave this for future work.

TABLE I
SUBMODULAR FUNCTION FOR QUALITATIVE EXAMPLE

	s_1	s_2	s_3	s_1, s_2	s_1, s_3	s_2, s_3	s_1, s_2, s_3
$f(\cdot)$	16	17	25	21	37	38	41

C. One Qualitative Example for DOL Framework

Let us consider a normalized submodular function f , i.e., $f(\emptyset) = 0$, defined over a ground set $\mathcal{S} = \{s_1, s_2, s_3\}$. Each element in \mathcal{S} can be viewed as a task route for UGVs. The values of f for choosing different elements are shown in Table I. Verifying the submodularity of f is easy using the definition in Section III. Each \mathcal{S} element is associated with a context-dependent cost. Suppose that the cost of s_3 is constantly to be one, and the ground truth costs for s_1 and s_2 are shown in Fig. 4a. We are interested in solving a problem as defined in Eq. (2) with $K = 2$. When we make decisions, we can only see the context, and we need to infer the route costs. The optimal decision is either $\{s_1, s_3\}$ or $\{s_2, s_3\}$. If we know the ground truth context-to-cost function as shown in Fig. 4a, the optimal decision boundary is $z = 4.45$ at which

TABLE II
TEST RESULTS OF OBJECTIVE VALUES

Training Parameters	DOL	two-stage	random
$n_a = 10, n_g = 3, N = 10$	200 ± 30	167 ± 26	80 ± 53
$n_a = 15, n_g = 5, N = 12$	320 ± 27	291 ± 27	100 ± 69
$n_a = 20, n_g = 7, N = 15$	470 ± 34	419 ± 23	220 ± 51

the cost choosing s_2 is greater than that of s_1 by 1. Namely, if the context observation z is less than 4.45, we should choose s_2 and s_3 . When z exceeds 4.45, we should choose s_1 and s_3 . Next, let us look at the result if learning is involved. We want to find a mapping from the observation z to costs. Suppose we obtain the training data by sampling from the ground truth as shown in Fig. 4a. MSE as the objective for learning without considering the downstream task, we will get two lines as shown in Fig. 4b. The decision boundary (dashed vertical red line, $z^* = 3.64$, at which $w_2 - w_1 = 1$) is on the left of the optimal boundary, thus not optimal. By contrast, if we consider the downstream optimization, we will get two lines as shown in Fig. 4 and the decision boundary (dashed vertical blue line, $z^* = 3.96$, at which $w_2 - w_1 = 1$) is closer to the optimal boundary, thus reducing the regions of suboptimal decisions.

D. Learning Loss over Epochs

We use a three-layer neural network to approximate the mapping g_θ . The number of parameters in the neural network will vary according to the number of UAVs (n_a) and the number of routes (N). In training, we use MSE loss first for a few epochs to as a warm start. Then, we will use DOL loss defined in Eq. (8). Fig. 6 shows one typical learning curve using the DOL loss over epochs. The loss will decrease first and reach a steady value, which suggests that the decision quality gap between the reference solution and the one obtained using predictions from g_θ is decreasing.

E. Comparison with Baseline

After training, we test the performance of the learned models using the simulator. We generate a set of context

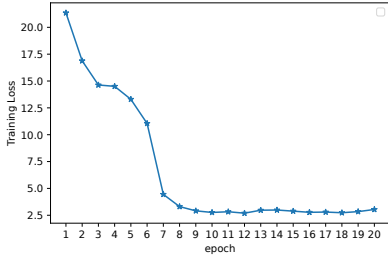


Fig. 6. Per epoch loss curve of DOL.

observations $\{z_i\}_{\text{test}}$ and compute the corresponding predicted weights $\{\hat{w}_i\}_{\text{test}}$. Then, we use $\{\hat{w}_i\}_{\text{test}}$ to select routes and feed the route to the simulator to obtain the actual intervention time and the coverage value. Then, we will use these two values to compute the objective value as defined in (1). The result of the objective value is shown in Table II. We compare three approaches: DOL (our), two-stage (classic supervise learning with MSE loss), and random (select routes randomly without any learning). As shown in Table II, our approach, on average, can result in a more balanced route selection (trade-off between task coverage and intervention time) and get a higher objective value for the route selections.

VII. CONCLUSION

We propose a decision-oriented learning framework for a special class of routing problems. We first show how to formulate the learning problem in the context of the vehicle routing problem. Then, we show how to make (non-monotone) submodular maximization a differentiable layer by using the proposed D-CSG algorithm and the multilinear extension of the objective function. The proposed framework and formulation are validated through several case studies.

REFERENCES

- [1] D. Rojas Vitoria, E. L. Solano-Charris, A. Muñoz-Villamizar, and J. R. Montoya-Torres, "Unmanned aerial vehicles/drones in vehicle routing problems: a literature review," *International Transactions in Operational Research*, vol. 28, no. 4, pp. 1626–1657, 2021.
- [2] A. B. Asghar, S. L. Smith, and S. Sundaram, "Multi-robot routing for persistent monitoring with latency constraints," in *2019 American Control Conference (ACC)*. IEEE, 2019, pp. 2620–2625.
- [3] B. Wilder, B. Dilkina, and M. Tambe, "Melding the data-decisions pipeline: Decision-focused learning for combinatorial optimization," in *Proceedings of the AAAI Conference on Artificial Intelligence*, vol. 33, no. 01, 2019, pp. 1658–1665.
- [4] A. Ferber, B. Wilder, B. Dilkina, and M. Tambe, "Mipaal: Mixed integer program as a layer," in *Proceedings of the AAAI Conference on Artificial Intelligence*, vol. 34, no. 02, 2020, pp. 1504–1511.
- [5] J. Mandi, P. J. Stuckey, T. Guns *et al.*, "Smart predict-and-optimize for hard combinatorial optimization problems," in *Proceedings of the AAAI Conference on Artificial Intelligence*, vol. 34, no. 02, 2020, pp. 1603–1610.
- [6] G. Shi and P. Tokekar, "Decision-oriented learning with differentiable submodular maximization for vehicle routing problem," *2023 IEEE/RSJ International Conference on Intelligent Robots and Systems (IROS)*, 2023.
- [7] Y. Bengio, A. Lodi, and A. Prouvost, "Machine learning for combinatorial optimization: a methodological tour d'horizon," *European Journal of Operational Research*, vol. 290, no. 2, pp. 405–421, 2021.
- [8] G. L. Nemhauser, L. A. Wolsey, and M. L. Fisher, "An analysis of approximations for maximizing submodular set functions—I," *Mathematical programming*, vol. 14, pp. 265–294, 1978.

- [9] S. M. Nikolakaki, A. Ene, and E. Terzi, "An efficient framework for balancing submodularity and cost," in *Proceedings of the 27th ACM SIGKDD Conference on Knowledge Discovery & Data Mining*, 2021, pp. 1256–1266.
- [10] N. Mathew, S. L. Smith, and S. L. Waslander, "Multirobot rendezvous planning for recharging in persistent tasks," *IEEE Transactions on Robotics*, vol. 31, no. 1, pp. 128–142, 2015.
- [11] P. Maini and P. Sujit, "On cooperation between a fuel constrained uav and a refueling ugv for large scale mapping applications," in *2015 international conference on unmanned aircraft systems (ICUAS)*. IEEE, 2015, pp. 1370–1377.
- [12] B. Amos and J. Z. Kolter, "Optnet: Differentiable optimization as a layer in neural networks," in *International Conference on Machine Learning*. PMLR, 2017, pp. 136–145.
- [13] A. Agrawal, B. Amos, S. Barratt, S. Boyd, S. Diamond, and J. Z. Kolter, "Differentiable convex optimization layers," *Advances in neural information processing systems*, vol. 32, 2019.
- [14] S. Muntwiler, K. P. Wabersich, and M. N. Zeilinger, "Learning-based moving horizon estimation through differentiable convex optimization layers," in *Learning for Dynamics and Control Conference*. PMLR, 2022, pp. 153–165.
- [15] B. Amos, I. Jimenez, J. Sacks, B. Boots, and J. Z. Kolter, "Differentiable mpc for end-to-end planning and control," *Advances in neural information processing systems*, vol. 31, 2018.
- [16] S. Chen, K. Saulnier, N. Atanasov, D. D. Lee, V. Kumar, G. J. Pappas, and M. Morari, "Approximating explicit model predictive control using constrained neural networks," in *2018 Annual American control conference (ACC)*. IEEE, 2018, pp. 1520–1527.
- [17] M. Bhardwaj, B. Boots, and M. Mukadam, "Differentiable gaussian process motion planning," in *2020 IEEE international conference on robotics and automation (ICRA)*. IEEE, 2020, pp. 10 598–10 604.
- [18] M. V. Pogančić, A. Paulus, V. Musil, G. Martius, and M. Rolinek, "Differentiation of blackbox combinatorial solvers," in *International Conference on Learning Representations*, 2019.
- [19] J. Djolonga and A. Krause, "Differentiable learning of submodular models," *Advances in Neural Information Processing Systems*, vol. 30, 2017.
- [20] S. Sakaue, "Differentiable greedy algorithm for monotone submodular maximization: Guarantees, gradient estimators, and applications," in *International Conference on Artificial Intelligence and Statistics*. PMLR, 2021, pp. 28–36.
- [21] C. Harshaw, M. Feldman, J. Ward, and A. Karbasi, "Submodular maximization beyond non-negativity: Guarantees, fast algorithms, and applications," in *International Conference on Machine Learning*. PMLR, 2019, pp. 2634–2643.
- [22] E. Jang, S. Gu, and B. Poole, "Categorical reparametrization with gumbel-softmax," in *International Conference on Learning Representations (ICLR 2017)*. OpenReview. net, 2017.
- [23] J. Seguro and T. Lambert, "Modern estimation of the parameters of the weibull wind speed distribution for wind energy analysis," *Journal of wind engineering and industrial aerodynamics*, vol. 85, no. 1, pp. 75–84, 2000.
- [24] T. Horel and Y. Singer, "Maximization of approximately submodular functions," *Advances in neural information processing systems*, vol. 29, 2016.
- [25] F. B. Sorbelli, F. Corò, S. K. Das, and C. M. Pinotti, "Energy-constrained delivery of goods with drones under varying wind conditions," *IEEE Transactions on Intelligent Transportation Systems*, vol. 22, no. 9, pp. 6048–6060, 2020.
- [26] G. Shi, N. Karapetyan, A. B. Asghar, J.-P. Reddinger, J. Dotterweich, J. Humann, and P. Tokekar, "Risk-aware uav-ugv rendezvous with chance-constrained markov decision process," in *2022 IEEE 61st Conference on Decision and Control (CDC)*. IEEE, 2022, pp. 180–187.
- [27] A. B. Asghar, G. Shi, N. Karapetyan, J. Humann, J.-P. Reddinger, J. Dotterweich, and P. Tokekar, "Risk-aware recharging rendezvous for a collaborative team of uavs and ugv," in *2023 IEEE International Conference on Robotics and Automation (ICRA)*. IEEE, 2023, pp. 5544–5550.
- [28] G. Özcan, A. Moharrer, and S. Ioannidis, "Submodular maximization via taylor series approximation," in *Proceedings of the 2021 SIAM International Conference on Data Mining (SDM)*. SIAM, 2021, pp. 423–431.